COBEM 2021 26th International Congress of Mechanical Engineering
ABCM Associação Brasileira de Engenharia e Ciências Mecânicas
November 22-26, 2021, Virtual Congress, Brazil

COB-2021-1430
EFFECT OF THE CARBON DIOXIDE CONCENTRATION AND THE PREHEATING OF REACTANTS ON THE COMBUSTION OF LOW CALORIFC VALUE BIOGAS MIXTURES
26th COBEM

José Alexandre de Campos
Roberto Wolf Francisco Jr.
State University of Santa Catarina, Department of Mechanical Engineering, Joinville - SC, Brazil
jose.campos@edu.udesc.br
roberto.francisco@udesc.br

Abstract. *Syngas and biogas are renewable fuels that have a minor impact over the environment, when compared to fossil fuels. Syngas are usually composed by CH_4, CO, H_2, and CO_2, depending on the raw material utilized in the gasification processes. Instead, biogas is produced by the anaerobic action of bacteria over biological waste and is composed mainly of CH_4 and CO_2, with traces of other gases. However, the composition of biogas can vary continuously during the production process, sometimes more abruptly and making it difficult to use it in conventional burners. Thus, the objective of this study is to evaluate the effect of the biogas composition and the preheating of the reactant's mixtures on the flame stability range, reaction temperature and radiation efficiency. The biogas used is compost by CH_4 and CO_2. The maximum concentration of CO_2 present in the fuel mixture, keeping the stable flame, will be determined experimentally, using a porous radiant burner. This type of burner was chosen for the present study due to the heat recirculation inside the porous matrix, which allows to achieve higher combustion rates and high reaction temperatures. Results using pure methane resulted in an equivalence ratio range between 0.45 and 0.55, for the reactants temperature at 300 K and pressure at 1 atm. The maximum equivalence ratio is limited by the degradation temperature of the porous ceramic used to build the burner (~1673 K). For the equivalence ratio equal to 0.5, the maximum thermal power obtained was 1.4 kW.*

Keywords: *Biogas; radiant porous burner, reactants preheating.*

1. INTRODUCTION

In recent times, there was an increase in the development of new types of fuel. This can be attributed to two main conditions, the first is environmental aspect, and the fact that the burning of fossil fuels are considered the main culprit of greenhouse gases emissions, the second point can be attributed to the world continuous growth of energy demand.

Syngas is a promising an alternative fuel, that can be obtained from steel production, in thermal gasification of biomass or coal and from municipal waste landfill (Arrieta et al., 2017). Jensen et al. (2007), demonstrated that is possible to produce syngas utilizing electric energy on an oxide electrolyser cell, transforming $CO_2 + H_2O$ into $CO + H_2$. Syngas is usually composed by hydrogen gas – H_2, carbon monoxide – CO, nitrogen gas – N_2 – and carbon dioxide – CO2, the N_2 and CO_2 gases acts as diluent in the fuel composition as they are inert gases.

Biogas is obtained from the anaerobic digestion of organic matter. According to Devi et al. (2020), biogas is mainly composed by methane gas – CH_4 – and carbon dioxide – CO_2 – with trace amounts of nitrogen – N_2, hydrogen sulfide – H_2S, carbon monoxide – CO, ammonia – NH_3, oxygen -O_2, hydrogen – H_2, water vapor – H_2O, dust and siloxanes. Biogas composition may vary according to its origin.

Janssens-Maenhout et al. (2019), explains that in the period from 1970 to 2012, the methane gas was the second most emitted greenhouse gas, and most of its emissions came from fermentation process like livestock manure, rice production, waste landfills and from diffusion process, coal mines and gas distribution leakages. Therefore, harnessing the methane, in the form of biogas, that otherwise would naturally be release to the atmosphere due to human activities, is a way to mitigate the emissions greenhouse gases utilizing a renewable energy source.

Syngas and biogas are fuels with low calorific values, and according to Arrieta et al. (2017), these aspect from those types of fuel can lead to problems associate with flame stability, combustion efficiency and reliability, on conventional technologies. One way to contour these difficulties is to utilize a radiant porous media burner. In this type of burner, the combustion occurs submerged, inside a porous matrix. The presence of solid matrix favors the occurrence of heat recirculation, that allows the preheating of the air-fuel mixture before it reaches the reaction zone, providing higher combustion rates and reactions temperatures.

Mujeebu et al. (2009) describes two major approaches to the design of a porous media combustion, the first where the combustion zone stays stationary inside the porous matrix, commonly used in radiant burner due to the solid high radiation

emission, and the transient approach where the combustion zone can move thru the porous matrix according to the energy fluxes. This second way leads to excess enthalpy flame theory, where the reagents are preheated by the burned fuel mixture, thus making possible to the system combustion temperature be higher than the theoretical adiabatic flame temperature. Still according to Mujeebu et al. (2009), there are several applications being studied and already in use for porous media burners, ranging from heat exchangers, oil and gas recovery, lighting, hydrogen production, combustion of low calorific value fuels, micro and meso-scale applications.

Yu et al. (2013) evaluates the emissions of CO and NO_x, in a boiler, for different types of materials constituting the porous matrix of the burner: metal fiber, ceramic and stainless-steel fin. The burner was tested with equivalence ratios from 0.8 to 0.95 and a capacity between 15 and 25 kW. In this work, the CO emissions and the NO_x decreases with greater porosity value, and the thermal efficiency is reduced for the smaller porosity. Chalia et al. (2020) made an extensive overview about the materials used and concluded that it has a significant importance in terms of performance and efficiency at a wide range of conditions, with ceramics materials showing potential to replace metallic material used in burners. Also, most of the ceramics utilized in the studies are based on oxides e carbide compounds, leaving research opportunities for different ceramic materials.

Keramiotis et al. (2012) tested a two-layer porous burner with equivalence ratios ranging from 0.625 and 0.83 and thermal loads between 200 and 1000 kW/m², burning CH4 and liquefied petroleum gas (LPG). The results showed that the burner presented a good fuel flexibility, achieving a stable combustion for a wide range of operation conditions, thermal loads and equivalence ratios, with low emissions. Also, was observed that the thermal load has more importance than the equivalence ratio, for the burner operation.

Gao et al. (2013) investigated the effects of the addition of inert gases, $CO_2 – N_2 – Ar$ to CH_4 using a radiant porous media burner. The inert gases varied from 25% to 40% in volume, with the equivalence ratios between 0.75 and 0.95. The results obtained show that the dilution of CO_2 reduces the flame stability limits more than with N_2 and Ar, this was attributed to the higher heat capacity of CO_2. In addition, for the CO2 dilution, it was observed that the flame position moved downstream with a higher flame speed, obtaining greater radiation efficiency than the mixtures with the other diluents. Also, it was observed that the presence of inert gas did not affect the emission levels of hydrocarbons.

Keramiotis et al. (2015) utilized CH_4, CO, H_2 and CO_2 to prepare the fuel mixtures, to simulate natural gas, biogas and syngas to burn in a radiant porous burner, with the thermal loads varying from 200 e 800 kW/m² and the excess air ratios between 1.1 and 1.8. It was observed that the addition of CO, H_2 and CO_2 to the fuel increase the CO emissions level, especially at higher thermal loads. But for low thermal loads, those emission were lower than 30 ppm, and the NOx emissions decreases with the leaner fuel mixtures. Subsequently, this study showed that fuel mixtures have an impact on the burner's radiation performance, with the fuel mixture composed of $CH_4/H_2/CO$ in equimolar proportions having the highest radiation efficiency, whereas the mixture with CO_2 in the fuel had a negative impact on the radiation efficiency.

Francisco Jr. et al (2010) evaluate hydrogen-rich gas fuel in a porous burner. It was observed that the addition of H_2 content in the fuel mixture, increase the stable combustion limits and wider the range of thermal power and operation of the burner, while the pollutant emissions decreases. It was determined that there was a reduction in the radiation efficiency with higher quantities of H_2 in the fuel mixtures, due to the movement of the flame front along the porous medium, with the addition of H_2 the flame front tends to approach the injection plate.

Song et al. (2017), analyzed radiant porous burner with annular heat recirculation, consisting of two concentric tubes, using an ultra-low calorific gas fuel, with heating values varying from 1,4 to 3,0 MJ/m³ compost by a mixture of CH_4 and N_2. It was observed that the increase in the low calorific value expands the stable combustion region, at the same time as it reduces CO emissions, and the pre-heating of the reactants contributes to the combustion of fuel with low calorific value.

Recently, Maznoy et al. (2021) analyzed an annular cylindrical radiant burner, operating with thermal power between 160 and 420 kW/m² and equivalence ratios of 0.5 to 1.0, using NG and NG-CO-H_2 blends as fuel. The researchers noted that the radiation operation region can be expanded to leaner equivalence ratios by the addition of H_2 in the fuel blend, without incurring in radiation efficiency loses.

An experimental and numerical analysis was conducted by Wang et al. (2019), to evaluate the effect of air preheating on flame stability, using a porous alumina medium. It was observed that the flame front moves upstream while its velocity and inclination decrease with the heating of the air-fuel mixture, attributing this to the higher enthalpy level of the mixture, and with that less heat needs to be absorbed from the porous matrix to the mixture reaches its ignition point, making easier to start the combustion reaction moving the flame front position upstream. The results show that the flame speed decreases as the air fuel mixture temperatures increases.

In view of the current aspects of studies carried out with low calorific value fuels, the present work focuses on the experimental analysis of the combustion of biogas, simulated with a mixture of methane (CH_4) and carbon dioxide (CO_2), using a radiant porous burner. The influence of the presence of CO_2 and the preheating of reagents on flame stability, thermal power range and radiation efficiency will be evaluated.

2. EXPERIMENTAL SETUP AND METHODOLOGY

2.1 Experimental setup

Figure 1 shows the schematic diagram of the experimental apparatus used to carry out the tests. It can be divided into three main groups, the first is the fuel air supply system, the second is the radiant porous burner, and the third group is the data acquisition and processing system.

The air supply comes from a compressor system that is pressure regulated, filtered and dried, before being sent to the OMEGA FMA-2609A mass flow controller, with a maximum mass flow of 50 SLPM.

The CH_4 is stored in a high-pressure vessel, the methane used is 99.5% pure, from the pressure regulator it is sent to an Omega FMA-A2409 mass flow controller, with a maximum measuring range of 10 SLPM.

Similar to CH_4, CO_2 is obtained from a cylinder with a purity of 99.99%. A pressure regulator was used to reduce the pressure down to 1.5 bar and a mass flow controller was used to measure the mass flow (OMEGA FMA-A2307), which has a maximum flow capacity of 2 SLPM. All these fluids are then mixed in a position away from the radiant porous burner manifold, then led to it through a line 8 mm in diameter.

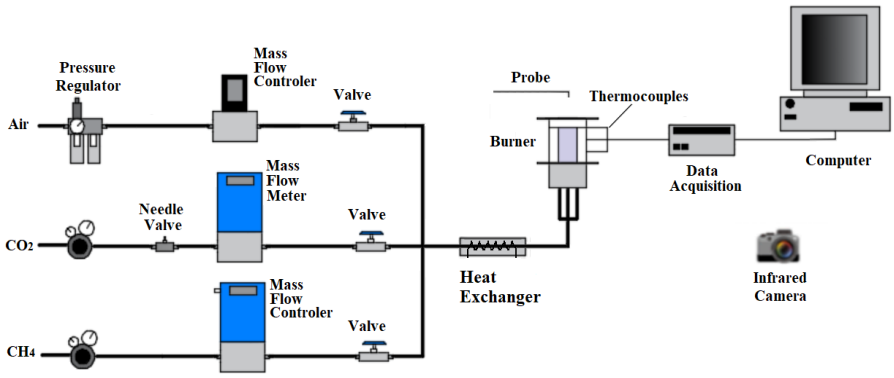

Figure 1. Radiant porous burner schematic drawing.

A typical two-layer porous burner design was used, similar to the one presented by Francisco Jr. *et al*. (2010). The burner was construct utilizing silicon carbide – SiC – foams as the porous medium. There are two distinct regions on the burner, the first region, upstream is preheating region – PR – is composed by porous medium with 20 ppi porosity, this higher porous density has a double purpose serving as a flame holder as well. The second region, downstream, is the stable burning region – SBR – and made by three porous medias with porosity of 10 ppi. Thus, the combustion region has a length of 80 mm and possess a diameter of 50 mm. Figure 2 shows the schematic of the burner and the thermocouples positions.

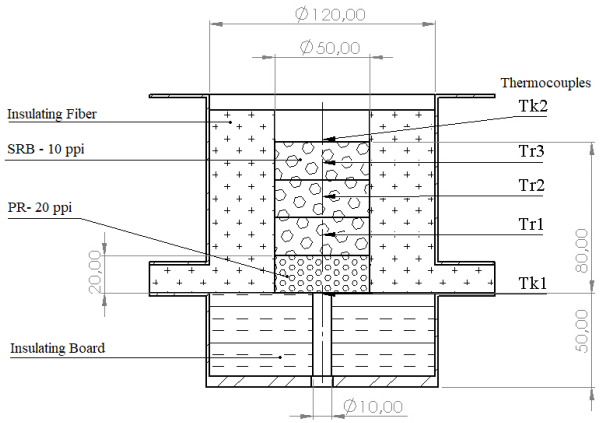

Figure 2. Radiant porous burner schematic drawing.

The thermocouples were positioned at the center of the burner, in the base, below of the first ceramic foam, a type K thermocouple is used. The thermocouples type R were employed downstream due to higher temperatures, with a ceramic coating to resist high temperature conditions. The surface temperature was measured utilizing a thermocouple type K and an infrared camera, FLIR model T650sc. Figures 3 shows the radiant porous burner in operation.

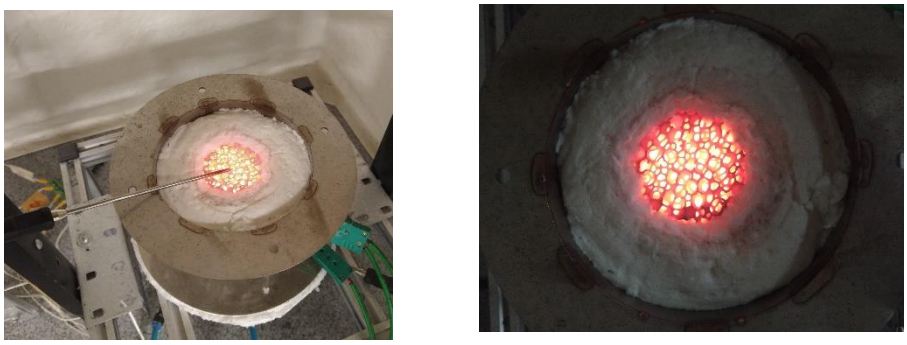

(a) (b)

Figure 3. (a) Radiant porous burner in operation and (b) close-up from the burner surface.

A data acquisition system (Keysight DAQ970A) was used with Benchvue software to monitor and record temperature readings. With these measurements it was possible to determine the temperature profile inside the burner, when the burner reaches stable operation and is operating in safe conditions. In addition, the Engineering Equation Solver software was used to calculate data inputs for mass flow controllers in order to achieve the desired equivalence ratios.

2.2 Parameter Definitions

The parameters utilized in this study are presented in the following equations, are well established in previous studies, as can be viewed in works from Francisco Jr. *et al*. (2010), Gao *et al.* (2013), Devi *et al.* (2020). Equation 1 presents the global combustion equation for biogas, as function of CO_2 mole fraction, α,

$$(1-\alpha)CH_4 + \frac{1+\phi}{\phi}(1-\alpha)(O_2 + 3.76N_2) + \alpha CO2 \rightarrow CO_2 + 2(1-\alpha)H_2O + 7{,}52(1-\alpha)N_2 + \frac{1+\phi}{\phi}(1-\alpha)(O_2 + 3.76N_2)\,. \quad (1)$$

The equivalence ratio, ϕ, is defined in Eq. 2,

$$\phi = \frac{(\dot{m}_{fuel}/\dot{m}_{air})_{ac}}{(\dot{m}_{fuel}/\dot{m}_{air})_{sto}}, \quad (2)$$

where $\dot{m}_{fuel}$ and $\dot{m}_{air}$ are the fuel mass flow rate and air mass flow rate, respectively, and the subscripts *ac* refers to the actual mass fuel ratio feed to the burner and *sto* to the stoichiometric mass fuel ratio. Eq. 3 and Eq. 4 displays in sequence the equation for the thermal power provided by the fuel and the radiation efficiency of the burner.

$$S_r = \dot{m}_{fuel} \cdot LHV, \quad (3)$$

$$\eta_{rad} = \frac{\varepsilon\sigma(T_{sur}^4 - T_{amb}^4)A_b}{S_r}, \quad (4)$$

where S_r is the thermal load, *LHV* is the fuel low heating value, η_{rad} is the radiation efficiency, ε is the emissivity of the burner, σ is Stefan-Boltzmann constant, A_b is burner surface area, *T* is the temperature with the subscripts *sur* and *amb*, referring to respectively, surface and ambient. For this study the emissivity of the burner was considered equals to 1.

Equation 5 presents the equation for uncertainty analysis, where UM_y is the measurement uncertainty of function *y*, UM_{xi} represents the uncertainty associated to each measurement system, $\partial y/\partial x_n$ is the partial derivative of function *y* regarding x_i measurement system and *n* is the total number of measurement systems.

$$UM_y = \sqrt{\sum_{i=1}^{n}\left(\frac{\partial y}{\partial x_i}UM_{xi}\right)^2}, \quad (5)$$

Table 1 presents the measurement uncertainties of the instruments used. Table 2 shows the results of uncertainty analysis calculated for the main parameters utilized in this study, thermal power and radiation efficiency.

Table 1. Measurement equipment uncertainties

Measurement Instrument	Uncertainty
CH4 mass flow controller FMA-A2409	± 1.0 % Full Scale
Air mass flow controller FMA-1600	± (0.8 % Reading + 0.2 % of Full Scale)
CO2 mass flow meter FMA-A2107	± 1.0 % Full Scale
Infrared Camera – Flir T650sc	± (1.0 ºC ± 1.0% of reading)
Thermocouples	± 2.0 ºC

Table 2. Uncertainty analysis

Parameter	Uncertainty
Thermal load - Sr	± 54.6 [W]
Radiation efficiency - η_{rad}	± 3.31 %

2.3 Experimental Procedure

The experimental procedure adopted for the study is similar to that presented by Francisco Jr. et al. (2010). The first step is to set up an equivalence relationship that allows igniting the fuel mixture. Subsequently, the reagent flows are adjusted to allow the flame front to propagate into the porous matrix, pre-heating it, until the thermocouple positioned at the base of the burner reaches a temperature close to 1000 ºC. Then, the operating point is adjusted, and the temperatures monitored to verify the flame propagation behavior inside the burner. A certain operating point is considered stable when the temperatures measured along the burner exhibit an almost constant behavior over a period of 20 minutes.

The upper limit of stability (or flame detachment) is defined as the operating point (equivalence ratio and flame velocity) at which the volumetric flow rate of the reactants is high enough to cause the flame front to detach from the surface of the burner. The lower stability limit occurs when the flame front moves to the base of the burner (near the injection plate), which can result in flame extinction or flashback. The flashback may occur when the temperature measured at the base of the burner is greater than 1100°C. The maximum allowable operating temperature has been limited to approximately 1673 K to prevent degradation of the porous material.

Table 3 shows the test conditions, with fuel compositions, initial reagent temperatures, and adiabatic flame temperature calculated using ANSYS Chemkin-Pro 18.2 software.

Table 3. Fuel mixtures and test conditions.

Fuel Composition [% vol.]	LHV [kJ/kg]	Equivalence Ratio	Reactants Temperatures [°C]	Adiabatic Flame Temperatures [K]
100 CH_4	50016	0.5	25	1751.5
72.5 CH_4 + 27.5 CO_2	24525			1722.0
72.5 CH_4 + 27.5 CO_2			60	1768.9

3. RESULTS AND DISCUSSIONS

3.1 Combustion reaction limits and burner temperature profile

This section presents the results obtained from tests utilizing methane, CH_4, as fuel to serve as a base line, and the results from a fuel mixture composed with 72.5% CH_4 and 27.5% CO_2. All tests were conduct with the same equivalence ratio of 0.5.

Initially, the stability limits for both mixtures and for the preheated condition were determined as can be seen in Figure 4. Pure methane presented a flame velocity range between 0.8 m/s and 0.44 m/s. For flame velocities below 0.8 m/s, flame extinction occurred, and the combustion reaction was not sustained. For velocity values above 0.44 m/s, the lift off limit has been reached, with the flame front being moved out of the porous medium, as shown in Figures 5a and 5b.

The fuel mixture containing CH_4/CO_2 showed an upper limit of stability similar to pure methane, with a maximum flame velocity of 0.44 m/s. However, the lower limit has been reduced to flame speed of 0.12 m/s. This can be attributed to the fact that CO_2 is a non-reactive component, acting as a diluent in the mixture, decreasing the reaction temperature and the thermal power for the same flame speed.

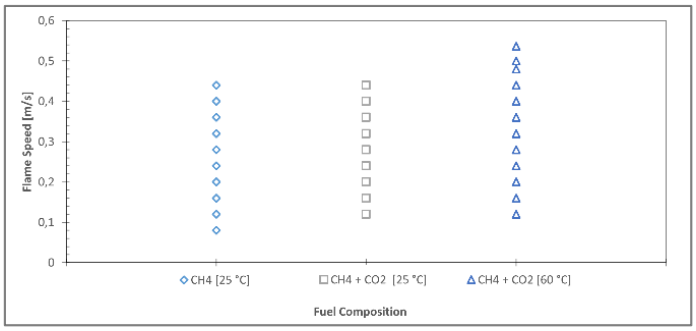

Figure 4. Stable combustion region for 100% CH_4, 72.5%CH_4 – 27.5%CO_2 and preheated 72.5%CH_4 – 27.5%CO_2.

In Figure 5a the flame starts to creep over the surface of the burner, moments later in Figure 5b, the flame front is above the burner surface.

(a) (b)

Figure 5. Blowout limits (a) Flame starts to move above burner surface, (b) Flame front out of the burner.

The temperature profiles for both configurations tested can visualized in Figures 6a, for the combustion of only methane, and in Figure 6b the fuel mixture containing 72.5% CH_4 and 27.5%C O_2. Figure 6 shows the effect of flame velocity on temperature measured by thermocouples positioned along the axis of the burner The higher temperatures represent the region where the combustion reaction occurs.

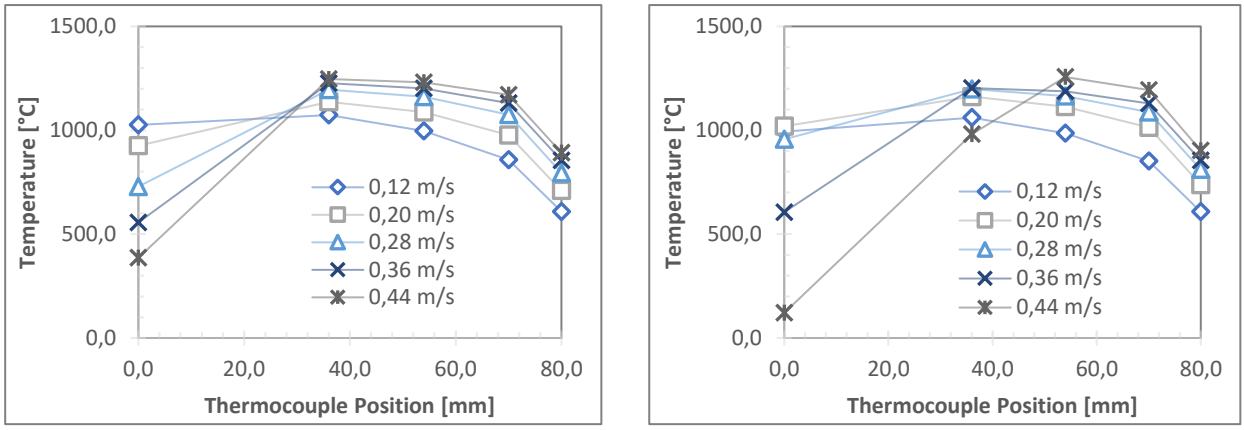

(a) (b)

Figure 6 – Temperature profiles as a function of the thermocouple position for (a) pure methane and (b) biogas at environment temperature.

Gao et al. (2012) comments that in a double-layer porous burner, the combustion reaction tends to occur near the interface where the porosity changes. Furthermore, this interface can act as a flame arrester, creating a restriction on the displacement of the combustion zone and reducing the possibility of flashback.

Comparing the two temperature profiles (Figures 6a and 6b), it was observed that the behavior is very similar for both fuels tested. As the flame speed increases, the thermal power supplied to the flame increases, but the volumetric flow injected into the burner also increases, displacing the flame front to the exit surface of the porous medium and reducing the temperature close to the injection plate.

For fuel mixture compost by CH_4 and CO_2 (Figure 6b), there is a significant reduction in the injection plate temperatures. For the highest flame speed of 0.44 m/s, the temperature measured was 120.9 °C, while that for pure metane (Figure 6a), the temperature for the same flame speed was 385.9 °C.

For the flame speed of 0.12 m/s for both fuels (see Figures 6a and 6b), pure methane showed a temperature close to the injection plate higher than the mixture with CH_4/CO_2. This effect is a result of the lower thermal power applied to the burner, resulting in the displacement of the flame front to a position near to the burner exit surface.

Another important aspect that can be observed in Figures 6a and 6b is the impact of flame velocity on the maximum temperature inside the porous burner. Thus, higher flame speeds result in higher temperatures due to the increased thermal power provided by the fuel mixture. For the highest flame velocities obtained for both fuels, the maximum measured temperatures were in the order of 1250°C.

3.2 Preheating effects of the fuel mixture

The biogas mixture (72.5% CH_4 - 27.5% CO_2) was preheated to a temperature of 60 °C to verify the effect of the preheating of the reactants over the burner operational conditions. As can be seen in Figure 4, the preheating of the fuel mixture increased the stability range of the burner, allowing it to operate with flame speeds between 0.12 m/s and 0.536 m/s. Comparing with the stability range obtained for this mixture at room temperature, it is noted that the lower stability limit was not changed, only the upper limit.

Figure 7a presents the temperature profiles for the different conditions tested, for a flame speed of 0.12 m/s and an equivalence ratio of 0.5. It is observed that the preheated mixture reached the highest temperature at the base of the burner, with a value of 1053.47 °C. For reagents at room temperature (pure methane and biogas), the maximum temperature was recorded in a thermocouple positioned 36.0 mm from the injection plate (burner base). In this position, CH_4 had a temperature of 1073.27 °C, slightly higher than the value measured for the CH_4/CO_2 mixture.

Figure 7b shows the temperature profile in the porous medium as a function of the burner length, for a flame speed of 0.44 m/s. It can be observed that the temperature measured at the base of the burner was lower for all conditions tested when compared with flame speed of 0.12 m/s (Figure 7a), showing the displacement of the flame front to the burner exit surface with increasing speed. The highest temperature measured (889.7ºC) at the base of the burner was for the biogas mixture preheated to 60ºC.

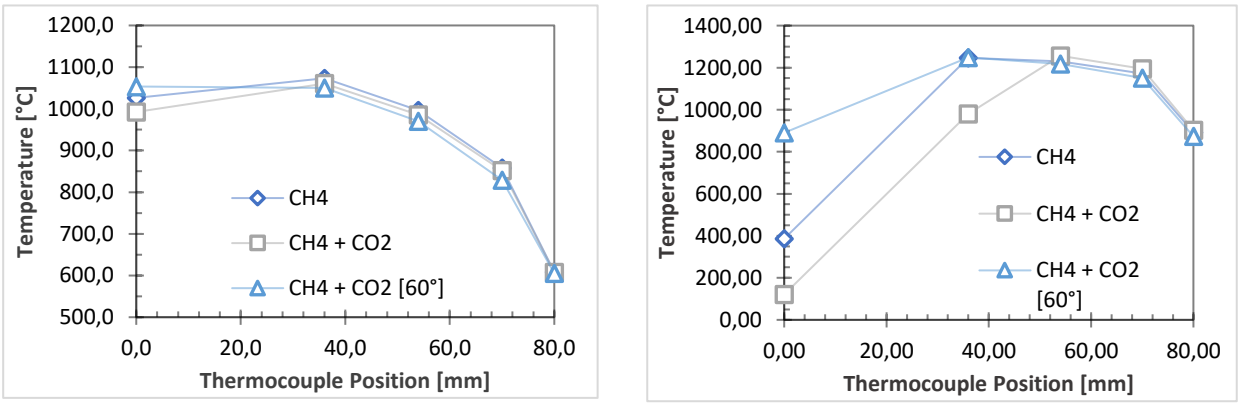

(a) (b)

Figure 7 – Temperature profiles as a function of the burner length for flame speed of (a) 0.12 m/s and (b) 0.44m/s.

3.3 Surface temperature and radiation efficiency

The surface temperature of the burner is important in determining the burner's radiation efficiency level. Although the presence of 27.5% CO_2 in the fuel composition has a negative impact on the low heating value of the fuel, reducing it from 50.0 MJ/kg (CH_4) to 24.5 MJ/kg (CH_4/CO_2), there were no significant changes in the temperatures recorded at the surface, as can be seen in Figure 8.

Figure 9 shows the burner surface temperatures measured using an infrared camera for all test conditions. It can be seen that the temperatures were very close, with a maximum difference of 10ºC between pure methane and the CH_4/CO_2 mixture at 60ºC. The determination of the radiation efficiency was determined using the average surface temperature obtained through FLIR Thermal Studio software.

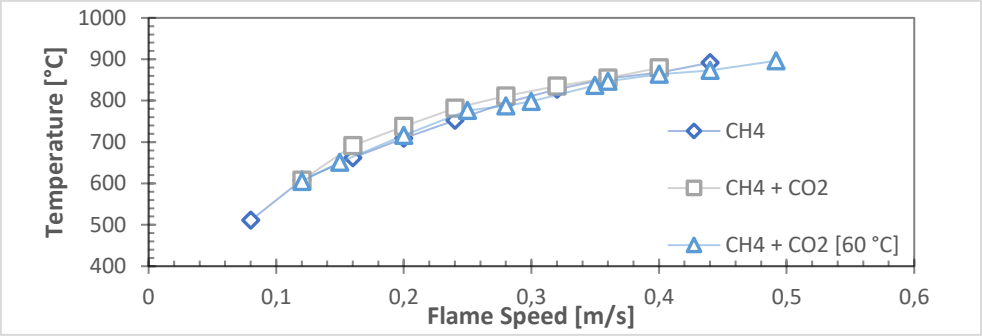

Figure 8. Burner surface temperatures.

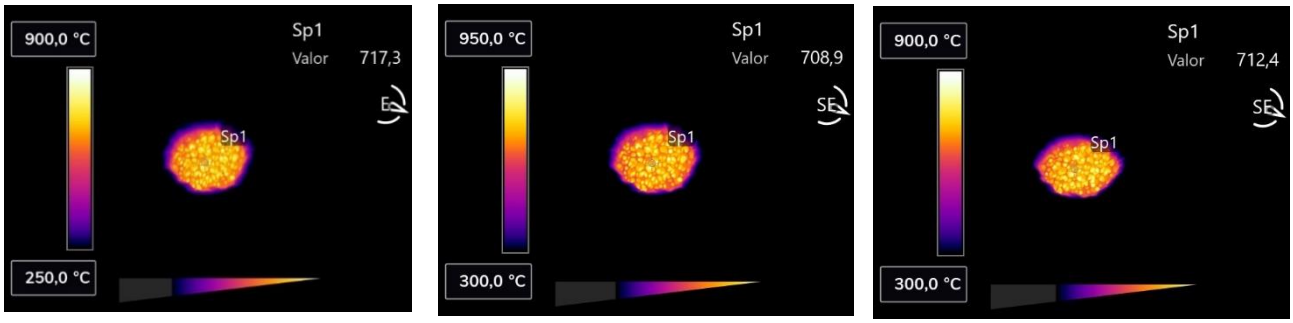

(a) (b) (c)

Figure 9. Infrared images of the burner with surface temperatures, flame speed 0.12 m/s, (a) 100 % CH_4, (b) 72.5% CH_4 – 27.5% CO_2 (c) 72.5% CH_4 – 27.5% CO_2 at 60 °C.

Figure 12 shows the radiation efficiency as a function of flame speed for all tested conditions. It can be noted that the results were similar for the two types of fuels tested, due to the low variation in surface temperature and thermal power supplied to the burner. For pure methane, the maximum efficiency was 17.16% for a flame speed of 0.12 m/s. As for the fuel mixture containing CO_2, the maximum radiation efficiency was 18.82% for a flame velocity of 0.16 m/s. This difference is within the estimated measurement uncertainty of 3.31%.

For the preheated fuel mixture, the radiation efficiency presented higher values, with the maximum efficiency of 19.21% for 0.12 m/s. This result may be related to the lower power supplied to the burner for a given flame speed, due to the reduction in the specific mass of the reactants and, therefore, in the mass flow of the fuel. Furthermore, it can be observed that for both types of fuel, even with preheating, the behavior of the efficiency curve was very similar, indicating an increase in efficiency with a reduction in flame speed.

This greater efficiency for the lowest surface temperature can be attributed, as mentioned by Devi et al. (2020), because the lower surface temperature is a consequence of the lower thermal power provided for the burner, this lower input power outcome is the reduction on the heat losses from the burner to the environment.

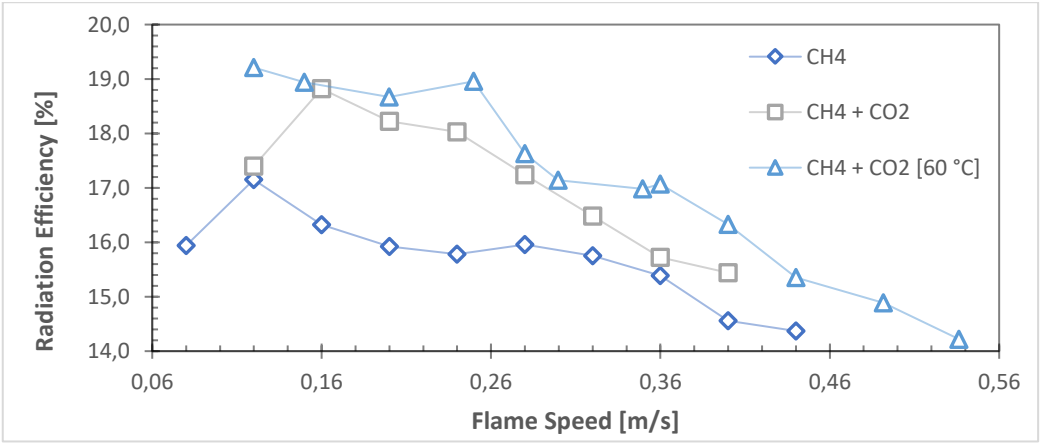

Figure 12. Radiation efficiency.

Arrieta *et al*. (2017) observed a decrease in radiation efficiency with the increase of the thermal load even though the surface temperatures roses, and suggests that the increase in gaseous phases speed, reduced the time the gases spent inside the radiant porous burner, thus not allowing the surface temperature to reach a value high enough that would permit the radiation level surpass the gain with the thermal load.

4. CONCLUSIONS

The radiant porous burner is an excellent solution for the combustion of low calorific value fuels. As shown in other studies, this type of burner has the ability to provide stable combustion over a wide range of operational conditions. The initial results obtained with the burner show that the increase in flame speed causes an increase in temperatures inside the burner, which may be associated with the increase in energy provided for the burner, caused by the greater flow of the reactants mixture. The higher flame velocity also causes the displacement of the combustion region inside the porous medium, with higher velocities resulting in the detachment of the flame front observed on the burner exit surface.

The preheating of the combustion reactants, results in a wider stability range of operation for the radiant porous burner tested, with maximum flame speed configuration registered of 0.54 m/s, above the values obtained for the reactants at ambient temperature, in which each achieve maximum flame speed configuration of 0,44 m/s.

As for the radiation efficiency, it was observed that the lowest flame speed reached the highest radiation efficiency. In agreement with other studies, this can be attributed to the fact that the increase in energy input does not only translate into higher surface temperatures of the radiant porous burner, due to the increase in heat loss from the burner to the environment. Furthermore, the higher flame speed reduces the time that the combustion gases remain inside the burner, causing a limitation in the heat transfer from the gases to the solid matrix, not allowing the surface temperature to reach a value where the radiation efficiency could be greater. The results for preheating of the combustion reactants over the radiation efficiency, showed higher values overall, when compared with the fuel without preheating, even though the results are still within the margin of error of the experiment.

The present study will continue in future, with further analysis considering different fuel compositions with higher CO_2 levels and distinct equivalence ratios and temperatures.

5. ACKNOWLEDGMENTS

The authors acknowledge the financial support of the Santa Catarina State Research and Innovation Foundation (FAPESC), Brazil, grant numbers 2017TR1748, 2017TR784 and 2019TR000779, and National Council for Research and Development (CNPq), Brazil, grant number 427885/2018-3. This study was financed in part by the Coordination for the Improvement of Higher Education Personnel (CAPES) - Finance Code 001.

6. REFERENCES

Arrieta, C. E., García, A. M., & Amell, A. A. (2017). Experimental study of the combustion of natural gas and high-hydrogen content syngases in a radiant porous media burner. International Journal of Hydrogen Energy, 42(17), 12669–12680. https://doi.org/10.1016/j.ijhydene.2017.03.078

Chalia, S., Bharti, M. K., Thakur, P., Thakur, A., & Sridhara, S. N. (2021). An overview of ceramic materials and their composites in porous media burner applications. Ceramics International, 47(8), 10426–10441. https://doi.org/10.1016/j.ceramint.2020.12.202

Devi, S., Sahoo, N., & Muthukumar, P. (2020). Experimental studies on biogas combustion in a novel double layer inert Porous Radiant Burner. Renewable Energy, 149, 1040–1052. https://doi.org/10.1016/j.renene.2019.10.092

Francisco Jr. R. W., Rua, F., Costa, M., Catapan, R. C., & Oliveira, A. A. M. (2010). On the Combustion of Hydrogen-Rich Gaseous Fuels with Low Calorific Value in a Porous Burner. 7, 880–887. https://doi.org/10.1021/ef9010324

Gao, H. Bin, Qu, Z. G., Tao, W. Q., & He, Y. L. (2013). Experimental investigation of methane/(Ar, N 2, CO 2)-air mixture combustion in a two-layer packed bed burner. Experimental Thermal and Fluid Science, 44(x), 599–606. https://doi.org/10.1016/j.expthermflusci.2012.08.023

Hashemi, S. M., & Hashemi, S. A. (2017). Flame stability analysis of the premixed methane-air combustion in a two-layer porous media burner by numerical simulation. Fuel, 202, 56–65. https://doi.org/10.1016/j.fuel.2017.04.008

Janssens-Maenhout, G., Crippa, M., Guizzardi, D., Muntean, M., Schaaf, E., Dentener, F., Bergamaschi, P., Pagliari, V., Olivier, J. G. J., Peters, J. A. H. W., Van Aardenne, J. A., Monni, S., Doering, U., Roxana Petrescu, A. M., Solazzo, E., & Oreggioni, G. D. (2019). EDGAR v4.3.2 Global Atlas of the three major greenhouse gas emissions for the period 1970-2012. Earth System Science Data, 11(3). https://doi.org/10.5194/essd-11-959-2019

Keramiotis, C., Katoufa, M., Vourliotakis, G., Hatziapostolou, A., & Founti, M. A. (2015). Experimental investigation of a radiant porous burner performance with simulated natural gas, biogas and synthes

Keramiotis, C., Stelzner, B., Trimis, D., & Founti, M. (2012). Porous burners for low emission combustion: An experimental investigation. Energy, 45(1), 213–219. https://doi.org/10.1016/j.energy.2011.12.006

Maznoy, A., Pichugin, N., Yakovlev, I., Fursenko, R., Petrov, D., & Shy, S. (Steven). (2021). Fuel interchangeability for lean premixed combustion in cylindrical radiant burner operated in the internal c

Mujeebu, M. A., Abdullah, M. Z., Bakar, M. Z. A., Mohamad, A. A., & Abdullah, M. K. (2009). Applications of porous media combustion technology - A review. Applied Energy, 86(9), 1365–1375. https://doi.org/10.1016/j.apenergy.2009.01.017

Muradov, N. Z., & Veziroğlu, T. N. (2008). "Green" path from fossil-based to hydrogen economy: An overview of carbon-neutral technologies. In International Journal of Hydrogen Energy (Vol. 33, Issue 23). https://doi.org/10.1016/j.ijhydene.2008.08.054

Rosa, R. (2017). The Role of Synthetic Fuels for a Carbon Neutral Economy. C, 3(4), 11. https://doi.org/10.3390/c3020011

Song, F., Wen, Z., Dong, Z., Wang, E., & Liu, X. (2017). Ultra-low calorific gas combustion in a gradually-varied porous burner with annular heat recirculation. Energy, 119, 497–503. https://doi.org/10.1016/j.energy.2016.12.077

Turns, S. R. (2012). An introduction to combustion: concepts and applications. Publisher McGraw-Hill, New York.

Wang, G., Tang, P., Li, Y., Xu, J., & Durst, F. (2019). Flame front stability of low calorific fuel gas combustion with preheated air in a porous burner. Energy, 170, 1279–1288. https://d

Yu, B., Kum, S. M., Lee, C. E., & Lee, S. (2013). Combustion characteristics and thermal efficiency for premixed porous-media types of burners. Energy, 53, 343–350. https://doi.org/10.1016/j.energy.2013.02.035

ZOU, C., XIONG, B., XUE, H., ZHENG, D., GE, Z., WANG, Y., JIANG, L., PAN, S., & WU, S. (2021). The role of new energy in carbon neutral. Petroleum Exploration and Development, 48(2), 480–491. https://doi.org/10.1016/S1876-3804(21)60039-3

7. RESPONSIBILITY NOTICE

The authors are the only responsible for the printed material included in this paper.